Augmented Fluid Surveillance Using Grid Sensing for Intelligent Transportation Service

Minsoo Kim, *Student Member, IEEE*, Jalel Ben-Othman, *Senior Member, IEEE*, and Hyunbum Kim, *Senior Member, IEEE*

***Abstract*—Recent vehicle cooperation is utilized for advanced missions, including next-generation communication and dynamic real-time information. active safety control for interconnected vehicles, collection of a heavy traffic information. In particular, the urban traffic surveillance should be one promising topic toward advanced vehicle road cooperation service supported by smart camera and Internet of Things (IoT). In this article, we introduce an augmented fluid surveillance system to create an adaptive fluid surveillance using a group of single lens cameras for intelligent transportation service. The research problem for augmented fluid surveillance is formally defined. Its objective is to optimize the surveillance efficiency for various traffic circumstances of traffic volumes so that the optimal deployment of smart camera is achieved. To settle the problem, two different methods are proposed with clear execution procedures and specifications. Then, their performances are evaluated with obtained results by extensive simulations for diverse settings and applicable scenarios. Furthermore, future research issues and works are described briefly.**

***Index Terms*—Augmented, fluid, surveillance, transportation, vehicle cooperation.**

I. Introduction

TRAFFIC management in smart cities is considered as a key element of sustainable urban development. The traffic sensing and management can be supported by various components, including Internet of Things (IoT), 5G and 6G communication technology, unmanned aerial vehicles (UAVs), and Industrial IoT [1], [2], [3], [4], [5], [6]. And, it can be utilized for various missions, including data handoff in edge computing, federated learning, trust-based certificate management, digital twin, and detecting compromised IoT components [7], [8], [9], [10], [11], [12], [13]. With the increasing traffic volume, the complexity of urban environments, the generalization of self-driving vehicles and the advent of connected equipment, the need for an efficient transportation system have become more important to be studied than ever [14], [15], [16], [17], [18]. It is highly anticipated that traffic monitoring can take a key role toward intelligent transportation service and vehicular networks in regard to autonomous vehicles, federated learning, generative AI, metaverse, and Industrial IoT [19], [20], [21], [22], [23], [24], [25], [26].

On the other hand, the surveillance should be a critical research branch because it can be used for numerous applications and essential tasks covering patrol service, terror threat prevention, criminal tracking, border surveillance, and so on [27], [28], [29], [30], [31], and [32]. Previously, the concept of barrier coverage was studied for surveillance purpose, including network intrusion detection, reconfigurable surveillance, virtual emotion-enabled surveillance, maritime transportation surveillance, etc [33]. In particular, the barrier coverage in traffic situations can be a very important factor in traffic management and safety. And, traffic monitoring barriers can play an essential role in ensuring the safety of vehicles and pedestrians, and keeping traffic flow smoothly. It reduces the risk of traffic accidents, prevents collisions between road users, while maintaining traffic order and promoting compliance with traffic laws. The barrier coverage is essential in taking prompt action in response to emergencies. For example, in the event of an accident, rapid rescue and emergency services may be provided with appropriate barrier coverage. In the traditional traffic management system, barrier coverage was mainly achieved through cameras or sensors installed in fixed locations. These static barriers were limited to specific areas, making it difficult to respond flexibly to changes in traffic volume. In addition, these systems might have limitations in reflecting the diversity of traffic conditions, especially in coping with rapid traffic changes or unexpected situations. Given surveillance system to generate an adaptive fluid surveillance using a group of single lens cameras, the existing study does not deliberate on the extensive evaluation with various scenarios covering different traffic volume, slope, and angle of camera for adaptive surveillance environment. Therefore, it is indispensable to study how to provide the augmented surveillance with efficient strategy according to an amount of traffic volume toward intelligent transportation service.

Then, based on the above observation, we give a concise summary for the main contributions of this article as follows.

1) An augmented surveillance model using grid sensing is introduced to create an adaptive fluid surveillance using a group of single lens cameras beyond the static surveillance by a single lens camera in existing traffic conditions.

Manuscript received 29 April 2024; revised 12 June 2024; accepted 22 June 2024. Date of publication 25 June 2024; date of current version 7 November 2024. *(Corresponding author: Hyunbum Kim.)*

Minsoo Kim and Hyunbum Kim are with the Department of Embedded Systems Engineering, Incheon National University, Incheon 22012, South Korea (e-mail: rlaalstn19@inu.ac.kr; hyunbumkim@ieee.org).

Jalel Ben-Othman is with the Université Paris-Saclay, CNRS, CentraleSupélec, Laboratoire des signaux et systémes, 91190 Gif-sur-Yvette, France, also with the University of Sorbonne Paris North, 93430 Villetaneuse, France, and also with the College of Technological Innovation, Zayed University, Abu Dhabi, UAE (e-mail: jbo@l2s.centralesupelec.fr).

Digital Object Identifier 10.1109/JIOT.2024.3419017

2327-4662 © 2024 IEEE. Personal use is permitted, but republication/redistribution requires IEEE permission.
See https://www.ieee.org/publications/rights/index.html for more information.

Authorized licensed use limited to: Univ Of Incheon. Downloaded on November 08,2024 at 08:11:11 UTC from IEEE Xplore. Restrictions apply.

2) The proposed system automatically activates or deactivates cameras according to changes in traffic volume, performs extensive monitoring during high-traffic situations, and a small range of monitoring during low-traffic circumstances.
3) Then, a main research problem is formally defined for augmented surveillance. Its goal is to maximize the sustainable efficiency with augmented surveillance according to various fluid traffic volume and status. Then, two different methods are devised to seek a solution of the problem, as well as are described with execution procedures and specifications.
4) The performances of the developed schemes are demonstrated through extensive simulations with several configurations, including different traffic volume, slope, and angle of camera.

The organization of this article consists of the following structure. In Section II, the previous works and the existing related works have been investigated for traffic monitoring and surveillance. In Section III, the assumptions, key terms, and problem definitions of the introduced system are specified. In Section IV, the proposed algorithms are specified to find a solution for the defined problem. Then, in Section V, we demonstrate the performance of the devised methods by expansive simulations with various settings and scenarios and provide discussions for obtained outcomes. And, this article is concluded in Section VI.

II. Related Works

There are numerous surveillance studies with various concentrations. Guo et al. [3] studied integrated network which covers security challenges, surveillance issues, and defense countermeasures in air and ground space. In [9], researchers investigated trust-enabled certificate administration for industry IoT networks to detect untrusted components, on-off attacks and then, provided security analysis against a party of potential security threats for compromised devices, denial-or-service, trusted related attacks. Zhu et al. [14] focused on the study of promising transportation systems to consider the mobility and dynamics of intelligent vehicles. Man et al. [17] deliberated on AI-assisted intrusion detection for intelligent Internet of vehicles, as well as suggested open issues for edge computing, federated learning, transfer learning, active defense, and privacy protection widely. Xiao et al. [20] introduced a federated learning system to provide self-motion traffic synthesis through multiple distributed generative adversarial networks. In [25], they studied vehicular digital twin networks for security and privacy with their solutions. Sarieddine et al. [28] proposed a real-time testbed with collaboration of multiple stakeholders and studied different cyberattack vectors in electric vehicle. In [29], they devised a deep learning system of radio surveillance that a fixed-wing drone is utilized for reliable radio surveillance. In [32], they designed a communication framework using dual-UAV for the surveillance among UAVs and ground elements. In [33], they introduced a secure framework to support differential surveillance by the generated security barriers in maritime transportation stations. Different from previous studies, this study presents a solution of how to support the adaptive fluid surveillance using a group of single lens cameras beyond the static surveillance in traffic management environment where reflects the diversity of traffic conditions or unexpected situations.

III. System Assumption and Problem Definition

Now, the system overview, assumption, key terms, and problem definitions are explained.

A. System Overview

The proposed system deliberated on the utilization of multiple single lens cameras to overcome the limitations of existing static surveillance barriers, enabling the system to adjust to varying traffic volumes. The proposed system automatically activates or deactivates cameras according to changes in traffic volume, performs extensive monitoring during high-traffic times, and a small range of monitoring during low-traffic times. Through this, it is expected to create augmented surveillance to adapt to fluid traffic conditions. The first landmark of the proposed system is to deploy and optimize single lens cameras effectively. Existing traffic management systems mainly focus on monitoring vehicles using single lens cameras, which have a difficulty in accurate detection due to the limitation of the vehicle's height or viewing angle in the event of an accident. As a solution to this, we utilize an three by three (3×3) array camera formation which is arranged at various heights and angles, providing an optimal viewing range to operate effectively in various vehicle types and traffic conditions. Also, the second objective of the proposed system is to seek a solution that dynamically controls the operation of the single lens camera according to changes in traffic volume. So, we proceed experiments using an arbitrary graph showing the characteristics of traffic volume by time-variant factor (i.e., the peak of traffic during morning rush hour, lunch, and evening rush hour). It is determined by analyzing the slope and changing speed of the traffic volume whether each camera is activated or not. Such a dynamic surveillance system shows that it is possible to create a flexible barrier according to the flow of traffic, which is different from an existing static system. For multifaceted analysis, the proposed system explores how the augmented surveillance system with a single lens camera that is dynamically adjusted according to traffic volume, as well as make a bridgehead to new opportunities for traffic management.

Fig. 1 depicts the examples of various traffic volume and monitoring situation through an arrangement of single lens cameras. Fig. 1(a) shows two single lens cameras are set up with different angles and directions when two traffic flows of vehicles on roads are given. Fig. 1(b) stands for the status of heavy traffic volume on roads where three by one array of single lens camera is located. And, Fig. 1(c) describes the status of low traffic volume on roads where three by one array of single lens camera is still positioned. As shown in Fig. 1, it is necessary to develop the adaptive surveillance strategy with

Authorized licensed use limited to: Univ Of Incheon. Downloaded on November 08,2024 at 08:11:11 UTC from IEEE Xplore. Restrictions apply.

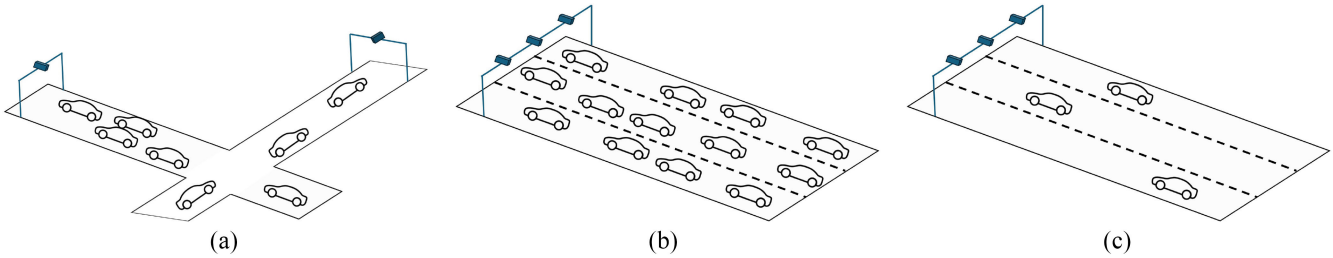

Fig. 1. Examples of various traffic volume and monitoring situation through smart camera. (a) Traffic situation for different directions. (b) Heavy traffic volume monitoring. (c) Low traffic volume sensing.

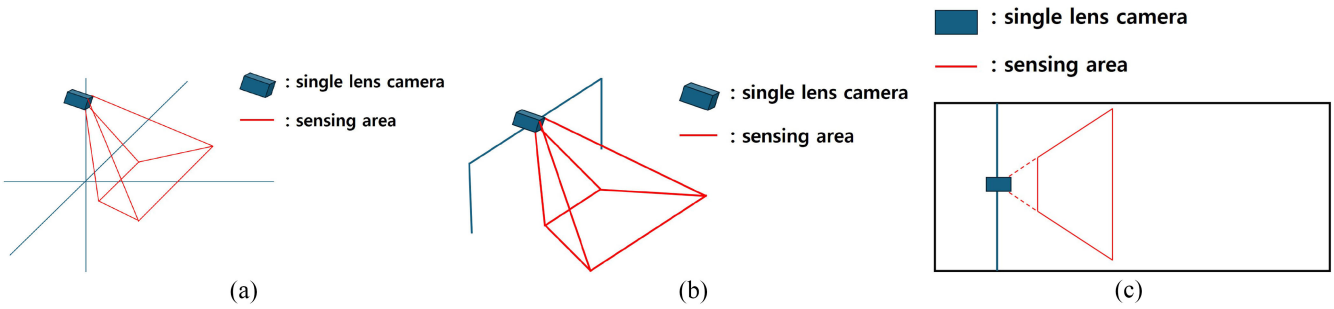

Fig. 2. Examples of single lens camera detection area with several circumstances and views. (a) Sensing area of single lens camera. (b) Sensing area in traffic situation. (c) Single lens camera activation with plan view.

energy and resource efficiency depending on traffic volume and conditions.

B. Assumption

Now, the assumptions which are used in the proposed system are specified.

1) The size of the traffic road is set up as 60 (width) × 30 (height) square-shaped area.
2) A single lens camera is installed in the air of the road. And, the single lens camera senses the objects within the detection range of the camera which has a fan-shaped sensing area with a radius of 10 and an angle of 60° when are viewed from top side.
3) Single lens cameras are not positioned in the equal location, but can recognize overlapping regions. And, they do not monitor off-road areas.
4) Single lens camera is placed with following the order of Level 1, Level 2, and Level 3 from the direction of traffic.
5) The proposed system utilizes time-variation traffic random graphs. Each graph has a maximum value depending on specific time. For example, 08:00 morning rush duration, 12:00 lunch hour, and 18:00 evening rush period.
6) In any given graph, the amount of traffic below a certain level is indicated as zero. It manages the power of single lens cameras at every 10 min.

C. Problem Definition

Then, a key term and a main research problem to be resolved are defined as follows.

Definition 1 (Augmented Fluid Surveillance): Suppose that there is the set of single lens cameras C, the set of random traffic flows T on the traffic road space S. The augmented fluid surveillance, called as *AugmentFluSurv*, is to provide augmented detection adaptively according to low traffic volume or heavy traffic fluid through the optimal assignment of cameras.

Definition 2 (Augmented Fluid Surveillance Efficiency Maximization Problem): Given that the set of single lens cameras C, the random traffic flows T on the traffic road space S, the augmented fluid surveillance efficiency maximization problem, referred as *MaxAugmentFluSurv*, is to maximize the resource efficiency with the minimum number of single lens cameras on condition that the requested surveillance through scale factor and base value is satisfied.

For the augmented fluid surveillance system with *AugmentFluSurv* using a group of single lens cameras for intelligent transportation service, the system purpose is to maximize the resource efficiency for the minimal number of single lens cameras on condition that *Sustain3DSurv* is accomplished with the generation of minimum number by the requested surveillance through scale factor and base value is met. And, we specify that the objective function (1) of *MaxAugmentFluSurv* problem is to

$$\textbf{Maximize } \alpha. \tag{1}$$

Fig. 2 shows The examples of single lens camera detection area with several circumstances and perspectives. Fig. 2(a) presents the sensing region or the detection area covered by single lens camera with 3-D view which is similar to pyramid shape. Fig. 2(b) simply depicts the sensing area of single lens camera which is equipped at traffic monitoring bar which generates the 3D-shaped detection space. Fig. 2(c) expresses

Authorized licensed use limited to: Univ Of Incheon. Downloaded on November 08,2024 at 08:11:11 UTC from IEEE Xplore. Restrictions apply.

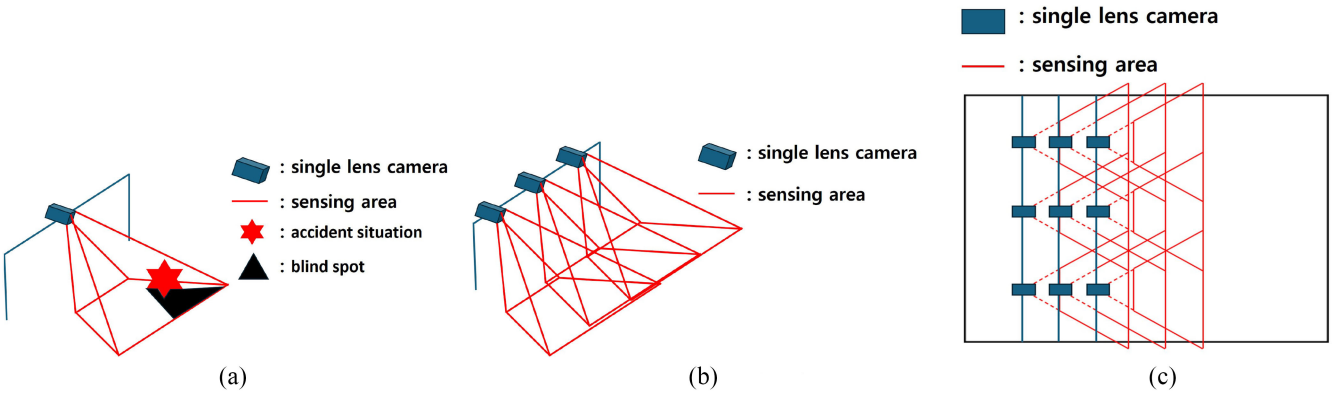

Fig. 3. Applicable scenario of single lens camera 3 × 3 array arrangement for detection area with various views. (a) Case of the blind spot due to accident situation. (b) 3 × 1 array with 3-D view. (c) 3 × 3 array with bird-eye view.

the status of single lens camera activation in traffic situation with plan view.

Fig. 3 depicts the applicable scenario of single lens camera 3 × 3 array arrangement for detection area with various views. Fig. 3(a) indicates the case of blind spot by the single lens camera because of an accident situation on traffic roads. Fig. 3(b) describes the state of sensing range with 3-D view when a single lens camera with 3 × 1 array is used for traffic roads. Furthermore, Fig. 3(c) represents the status of sensing range with bird-eye view when a single lens camera with 3 × 3 assignment strategy is applied properly.

IV. Proposed Schemes

In this section, the proposed methods to resolve the *MaxAugmentFluSurv* problem are specified. It is noted that the goal is to adjust the power of the single lens camera according to the graph with the linear features of the traffic situation and the graph with the curved features to create and cover the targeted traffic surveillance roads with more space when there is heavy traffic, and to reduce the area by creating fewer traffic surveillance roads. This goal can be achieved by combining straight and curved graphs to see if such a strategy can be applied to the actual traffic graph and whether the number of on/off cameras increases or decreases similar to the given situation. The study further develops two key approaches: One is based on *random value propagation by camera level* and another is achieved with *all random with weight value*. These approaches dynamically control camera operations in response to traffic volume changes, as demonstrated in graphs representing typical traffic patterns.

A. Initialization:Time-Variation-Graph-Creation

As a system initialization, the *Time-Variation-Graph-Creation* is performed, which generates two random types of graphs: Graph 1: *Linear-Graph* and Graph 2: *Curvature-Graph*. Two graphs have maximum values based on 8 o'clock in the morning, 12 o'clock in the afternoon, and 18 o'clock in the evening, respectively.

The Graph 1: Linear-Graph is a function that increases and decreases linearly from 2 h ago based on each maximum value. The slope of the function is fixed to 0.5 when the traffic increases and decreases by −0.5. Also, the Graph 2: *Curvature-Graph* is a function that increases and decreases along the curvature of the sin function from 2 h ago based on each maximum value. The corresponding function is a $\sin(1/4 \times \pi)$ function and represents the interval between 0 and π. Note that a random value is assigned to each single lens camera and the function of turning on the power when the value is less than the value of the graph defined above. The *base* is the minimum percentage of cameras in the graphs where the camera is always on except for the camera for essential sensing. Also, the $scale_{factor}$ is a function that scales the amplitude of the function. The power management of the camera can be performed only if the value of the function is fixed into a value between 0 and 1. If the base is set, it becomes the $scale_{factor}$ = (1 - *base*). This is because the maximum value of the function is 1 and a function graph is moved by the *y*-axis by the base, so the function must be applied in the area of the size of (1 - *base*).

Fig. 4(a) and (b) represent the movement rate of the vehicle changes with the variables $scale_{factor}$ and *base* for normal function. Also, Fig. 4(c) and (d) show the cases which $scale_{factor}$ = 0.5 and *base* = 0.5 are applied in Graph 1: *Linear-Graph* and Graph 2: *Curvature-Graph*.

B. Algorithm 1: Random-Value-Camera-Level

Note that the primary objective is the strategic deployment and optimization of single lens cameras for augmented fluid surveillance for dynamic traffic volume. So, we propose 3 × 3 array camera system, strategically arranged to cover diverse vehicle heights and angles, ensuring effective operation under various traffic conditions. Fig. 5 presents the placement of camera 1 through 9 according to vehicle direction based on 3 × 3 array camera system where each level consists of three number of single lens camera. As shown in Fig. 5, considering the nature of the traffic situation, Level 3 with cameras 1 through 3 is always supplied with power through the proposed algorithm processing to enable at least 1 fluid surveillance.

Also, the performed study showcases the potential of dynamic surveillance to adapt to traffic conditions, reducing unnecessary camera usage in low traffic situations. The use of $scale_{factor}$ and *base* values further refines the system's

Authorized licensed use limited to: Univ Of Incheon. Downloaded on November 08,2024 at 08:11:11 UTC from IEEE Xplore. Restrictions apply.

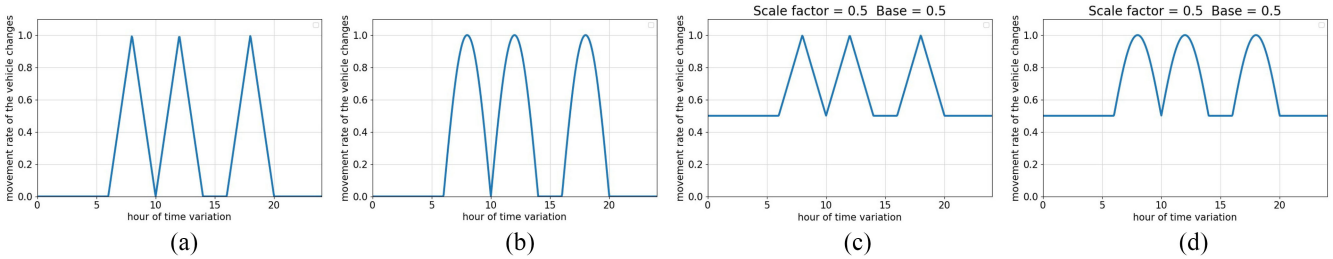

Fig. 4. Normal function according to the movement rate of the vehicle changes, $scale_{factor}$, *base* in Graph 1 and Graph 2 where X-coordinate: the hour of time variation and Y-coordinate: movement rate of the vehicle changes. (a) Movement rate of the vehicle changes linearly at 08 o'clock, 12 o'clock, and 18 o'clock for Graph 1: *Linear-Graph*. (b) Movement rate of the vehicle changes linearly at 08 o'clock, 12 o'clock, and 18 o'clock for Graph 2: *Curvature-Graph*. (c) Scale factor = 0.5 and base = 0.5 applied to Graph 1: *Linear-Graph*. (d) Scale factor = 0.5 and base = 0.5 applied to Graph 2: *Curvature-Graph*.

Algorithm 1 *Random-Value-Camera-Level*
Input: C, S, T, G Output: $|C_{\text{act}}|$

identify the traffic road space S;
verify the set of single lens camera C;
check the graph type G;
create the activated set of single lens camera C_{act};
assign 3×3 array camera system for C;
set $C_{\text{act}} \leftarrow \emptyset$;
set $C'_{\text{act}} \leftarrow \emptyset$;
while 24 hours is not elapsed **do**
    declare a random value R for every single lens cameras in C;
    subtract $0.5 \times scale_{factor}$ from the declared random value of Level 1 to obtain the values of Level 2 single lens cameras 4, 5, and 6;
    subtract $scale_{factor}$ from the declared random value of Level 1 to obtain the values of Level 3 single lens cameras 7, 8, and 9;
    estimate the number of cameras turned on c_n for a camera having a value smaller than the given graph G at every 10 minutes;
    set $C'_{\text{act}} \leftarrow C'_{\text{act}} \cup c_n$;
end while
calculate the average value and set it as $|C_{\text{act}}|$;
return $|C_{\text{act}}|$;

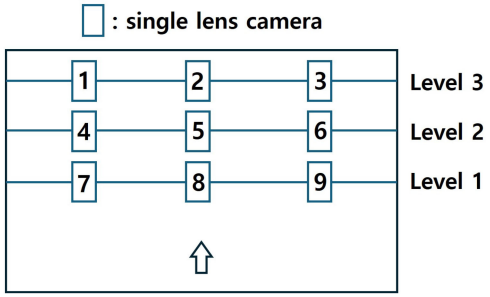

Fig. 5. Placement of camera 1 through 9 at each level.

responsiveness, allowing for efficient power management and barrier formation tailored to real-time traffic needs. This strategy not only advances traffic management strategies but also opens avenues for its application in various dynamic environments requiring augmented fluid surveillance.

Based on initialization, *Time-Variation-Graph-Creation* and above strategy, the first algorithm is devised, which is referred as *Random-Value-Camera-Level*. It is noted that the *MaxAugmentFluSurv* problem is to maximize the resource efficiency with the minimal number of single lens cameras such that the required surveillance through scale factor and base value is met. To resolve the issue, the basic idea of Algorithm 1: *Random-Value-Camera-Level* is to only assign random values to Level 1 cameras, propagating these values to cameras at the same column but with different weights at each level. This results in Level 3 maintaining a baseline barrier coverage, while Levels 1 and 2 adaptively expand coverage in accordance with traffic volume. That is, the Random value propagation by camera level method is a method in which only single lens cameras in Level 1 are given a random value, the random value is propagated to single lens cameras in the same column's Levels 2 and 3, and different weight values are applied to each level. If the corresponding value is smaller than the value of the graph enhanced by the $scale_{factor}$ and *base*, the camera is turned on. Level 2 has a weight of $-0.5 \times scale_{factor}$. If $-0.5 \times scale_{factor}$ is performed on random values propagated in leaves, the value may be greater or less than base, which manages sensor power for dynamic barrier coverage in level 2. The weight of Level 3 is $-scale_{factor}$. If you do $-scale_{factor}$ for any random value, it will be smaller than the base, and the camera of Level 3 will always be on. This will essentially result in line 1 barrier coverage at Level 3 and expand the area of fluid surveillance using the value of Level 1 to achieve additional fluid surveillance. Then, the pseudocode of Algorithm 1: *Random-Value-Camera-Level* is elucidated in Algorithm 1 in more detail.

C. Algorithm 2: ALL-Random-With-Weight

After initialization, *Time-Variation-Graph-Creation* and 3×3 array camera arrangement are performed, we propose the second algorithm, referred as *ALL-Random-With-Weight*. The essential idea of Algorithm 2: *ALL-Random-With-Weight* is to assign random values to each camera, with weight adjustments based on camera levels. Cameras at Level 3 are always active due to their weight being adjusted by the negative $scale_{factor}$. It follows that The all random with weight value method gives a random value to all cameras and a weight value to each level to which each camera belongs. If the corresponding value is smaller than the value of the

Authorized licensed use limited to: Univ Of Incheon. Downloaded on November 08,2024 at 08:11:11 UTC from IEEE Xplore. Restrictions apply.

Algorithm 2 *ALL-Random-With-Weight*
Input: C, S, T, G Output: $|C_{\text{act}}|$

confirm the traffic road space S;
certify the set of single lens camera C;
validate the graph type G;
generate the activated set of single lens camera C_{act};
arrange 3×3 array camera system for C;
set $C_{\text{act}} \leftarrow \emptyset$;
set $C'_{\text{act}} \leftarrow \emptyset$;
while 24 hours is not passed **do**
    ascertain a random value R for each single lens cameras in C;
    subtract $scale_{factor}$ from random value of cameras 1, 2, and 3 in Level 3;
    check the number of cameras turned on c_n for a camera having a value smaller than the given graph G at every 10 minutes to which $scale_{factor}$ and $base$ value are applied;
    set $C'_{\text{act}} \leftarrow C'_{\text{act}} \cup c_n$;
end while
compute the average value and decide it as $|C_{\text{act}}|$;
return $|C_{\text{act}}|$;

graph adjusted by the $scale_{factor}$ and $base$, the camera is turned on. The weight of Level 3 is $-scale_{factor}$. If $-scale_{factor}$ is considered for any random value, it will be smaller than the $base$, and the camera of Level 3 will always be on. Given random value R it is replaced with $scale_{factor} = 1 - base$ in $R - scale_{factor}$, that is, $R + base - 1$. Hence, any value R will be smaller or the same as the $base$. Levels 1 and 2 are not weighted, and this expands the area of Level 3's line 1 fluid surveillance barrier according to the change in the given graph G showing the change in traffic volume so that additional fluid surveillance barrier can be achieved.

Then, the pseudocode of Algorithm 2: *ALL-Random-With-Weight* is expounded in Algorithm 2 in more detail.

V. Experimental Evaluations

A. Numerical Result Analysis

In this section, the performances of the enlightened Algorithm 1: *Random-Value-Camera-Level* and Algorithm 2: *ALL-Random-With-Weight* are demonstrated. For the executed simulation environments, all simulations were operated by ad-hoc server with Window 11. The simulation program is coded by Python 3.9.13. The total number of single lens camera is 9 where its sensing range is 10 and the detection degree limit is set as 60° for each camera. The total number of experiments is 24(h) × (60(min)/10(min)) = 144 when 24 h is given. Fig. 6 shows the simulation setting environment which is composed of 3×3 array camera arrangement on traffic road whose size is 60 by 30. As a whole, the simulation sets consist of four different simulation scenarios and settings for the proposed schemes. It is analyzed for the composition of 9 single lens cameras in a 3×3 arrangement to achieve fluid surveillance according to the graph of traffic volume.

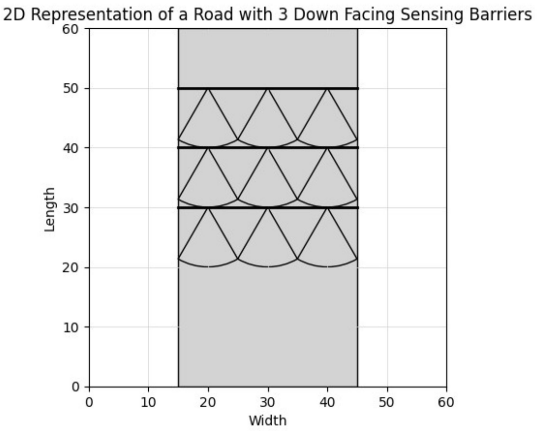

Fig. 6. 3×3 array camera arrangement on traffic road size with 60 by 30.

For the first set of experiments, Algorithm 1: *Random-Value-Camera-Level* is implemented by different $scale_{factor}$ and $base$ for Graph 1: *Linear-Graph*. At Fig. 7, the X-coordinate illustrates the hour of time variation and Y-coordinate stands for an activated number of single lens camera for augmented fluid surveillance. The dotted red line is about traffic volume depending on time variation per hour. The solid blue line is the result value of Algorithm 1: *Random-Value-Camera-Level*. Fig. 7(a) and (b) represent the output when $scale_{factor} = 0.7$ and $base = 0.3$ and $scale_{factor} = 0.8$ and $base = 0.2$ are given. Fig. 7(c) and (d) show the result if $scale_{factor} = 0.9$ and $base = 0.1$ and $scale_{factor} = 0.99$ and $base = 0.01$ are used. As shown in Fig. 7, it is demonstrated that Algorithm 1: *Random-Value-Camera-Level* shows the feasible efficiency to provide fluid surveillance according to various traffic volumes with time variation.

About the second group of simulations, Algorithm 1: *Random-Value-Camera-Level* is executed by various $scale_{factor}$ and $base$ for Graph 2: *Curvature-Graph*. Fig. 8 has the equal representation for X-coordinate, Y-coordinate, the dotted red line, and solid blue line, respectively. Then, Fig. 8(a) and (b) show the numerical result when $scale_{factor} = 0.7$ and $base = 0.3$ and $scale_{factor} = 0.8$ and $base = 0.2$ are put into the scenario. Also, Fig. 8(c) and (d) confirm the outcome if $scale_{factor} = 0.9$ and $base = 0.1$ and $scale_{factor} = 0.99$ and $base = 0.01$ are utilized in Graph 2: *Curvature-Graph*.

On the other hand, for the third set of experiments, we executed Algorithm 2: *ALL-Random-With-Weight* through several factors of $scale_{factor}$ and $base$ for Graph 1: *Linear-Graph*. Similar to previous settings, at Fig. 9, the X-coordinate depicts the hour of time variation and Y-coordinate presents the activated number of single lens camera, as well as the dotted red line is about traffic volume and the solid blue line is the output of Algorithm 2: *ALL-Random-With-Weight*. Fig. 9(a) and (b) verify the result when $scale_{factor} = 0.7$ and $base = 0.3$ and $scale_{factor} = 0.8$ and $base = 0.2$ are set up. Fig. 9(c) and (d) show the performance if $scale_{factor} = 0.9$ and $base = 0.1$ and $scale_{factor} = 0.99$ and $base = 0.01$ are utilized. As it can be seen in Fig. 9, it is checked that Algorithm 2: *ALL-Random-With-Weight* returns the adaptive results for fluid surveillance depending on traffic volume changes.

Authorized licensed use limited to: Univ Of Incheon. Downloaded on November 08,2024 at 08:11:11 UTC from IEEE Xplore. Restrictions apply.

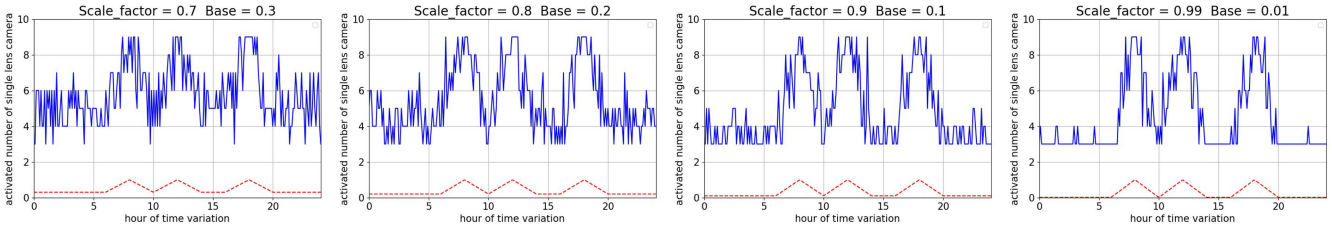

Fig. 7. Performance of Algorithm 1: *Random-Value-Camera-Level* with different $scale_{factor}$ and *base* for Graph 1: *Linear-Graph* where *X*-coordinate: the hour of time variation and *Y*-coordinate: the activated number of single lens camera. (a) $scale_{factor} = 0.7$ and $base = 0.3$. (b) $scale_{factor} = 0.8$ and $base = 0.2$. (c) $scale_{factor} = 0.9$ and $base = 0.1$. (d) $scale_{factor} = 0.99$ and $base = 0.01$.

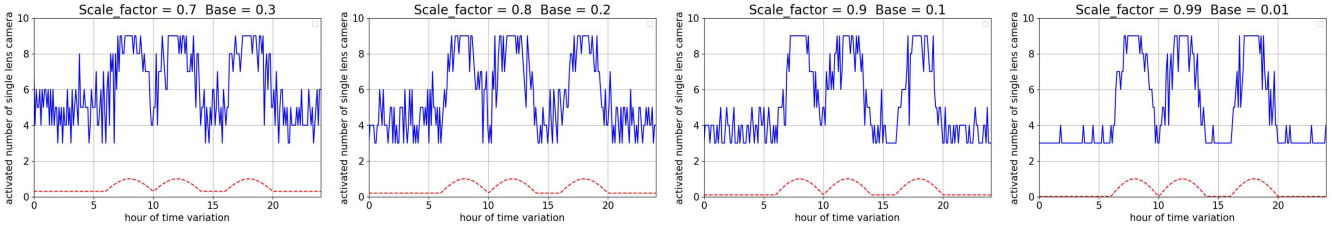

Fig. 8. Performance of Algorithm 1: *Random-Value-Camera-Level* with various $scale_{factor}$ and *base* for Graph 2: *Curvature-Graph* where *X*-coordinate: the hour of time variation and *Y*-coordinate: the activated number of single lens camera. (a) $scale_{factor} = 0.7$ and $base = 0.3$. (b) $scale_{factor} = 0.8$ and $base = 0.2$. (c) $scale_{factor} = 0.9$ and $base = 0.1$. (d) $scale_{factor} = 0.99$ and $base = 0.01$.

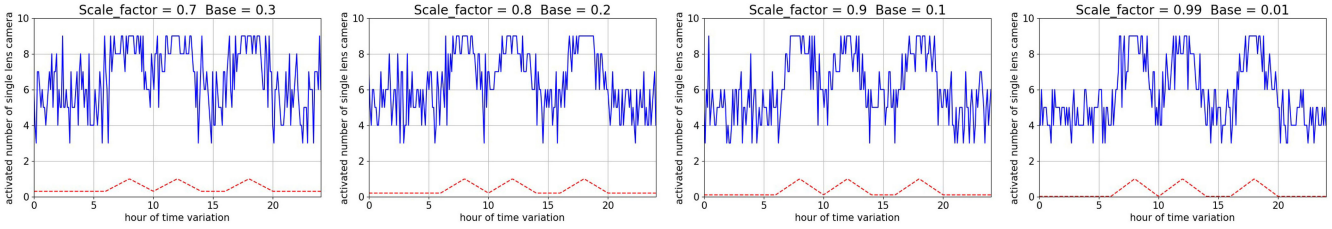

Fig. 9. Performance of Algorithm 2: *All-Random-With-Weight* through several factors of $scale_{factor}$ and *base* for Graph 1: *Linear-Graph* where *X*-coordinate: the hour of time variation and *Y*-coordinate: the activated number of single lens camera. (a) $scale_{factor} = 0.7$ and $base = 0.3$. (b) $scale_{factor} = 0.8$ and $base = 0.2$. (c) $scale_{factor} = 0.9$ and $base = 0.1$. (d) $scale_{factor} = 0.99$ and $base = 0.01$.

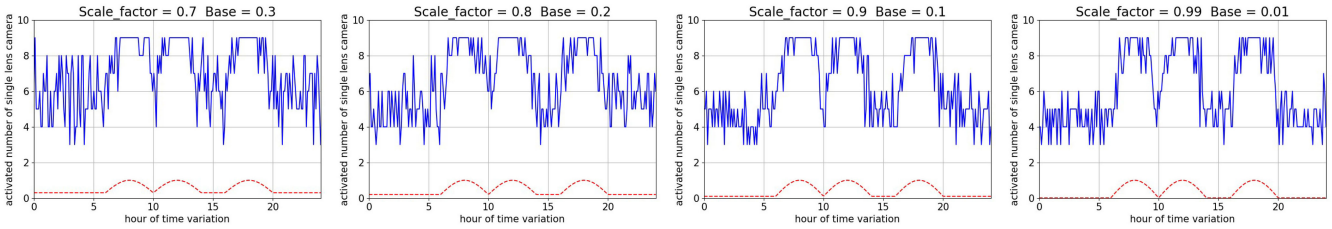

Fig. 10. Performance of Algorithm 2: *All-Random-With-Weight* with various $scale_{factor}$ and *base* for Graph 2: *Curvature-Graph* where *X*-coordinate: the hour of time variation and *Y*-coordinate: the activated number of single lens camera. (a) $scale_{factor} = 0.7$ and $base = 0.3$. (b) $scale_{factor} = 0.8$ and $base = 0.2$. (c) $scale_{factor} = 0.9$ and $base = 0.1$. (d) $scale_{factor} = 0.99$ and $base = 0.01$.

About the fourth group of scenarios, Algorithm 2: *ALL-Random-With-Weight* is accomplished by various $scale_{factor}$ and *base* for Graph 2: *Curvature-Graph*. Fig. 10 covers the same representation for *X*-coordinate, *Y*-coordinate, the dotted red line, and solid blue line. Fig. 10(a) and (b) turn up the output when $scale_{factor} = 0.7$ and $base = 0.3$ and $scale_{factor} = 0.8$ and $base = 0.2$ are entered. Fig. 10(c) and (d) are open to the view of the performance if $scale_{factor} = 0.9$ and $base = 0.1$ and $scale_{factor} = 0.99$ and $base = 0.01$ are given. As a whole set of experiments, it is verified that the power of the single lens camera is less unnecessarily turned on in low traffic situations as $scale_{factor}$ and *base* are adjusted. We can see that the lower value of *base* is desired to be turned on basically and the less unnecessary power is wasted in situations with less traffic. Furthermore, we demonstrate that Algorithm 1: *Random-Value-Camera-Level* has the advantage

Authorized licensed use limited to: Univ Of Incheon. Downloaded on November 08,2024 at 08:11:11 UTC from IEEE Xplore. Restrictions apply.

TABLE I
AVERAGE NUMBER OF SINGLE LENS CAMERAS USED PER 10 MIN FOR FOUR BASE VALUES IN REGARD TO TRAFFIC VOLUME WHEN THE PROPOSED ALGORITHMS ARE TESTED IN GRAPH 1: *Linear-Graph* AND GRAPH 2: *Curvature-Graph*

Alg\base	0.3	0.2	0.1	0.01
Alg1. Graph1	6.795	6.475	6.033	5.866
Alg1. Graph2	6.991	6.6625	6.3833	6.104
Alg2. Graph1	5.933	5.329	4.883	4.4475
Alg2. Graph2	6.158	5.695	5.266	4.904

of forming a fluid surveillance leading to Level 2 Level 1 from Level 3's perspective, but on average, it has the disadvantage of using more single lens cameras. On contrary, Algorithm 2: *ALL-Random-With-Weight* has the advantage of dynamically turning on and off the single lens camera where Level 3 generates 1 line of essential surveillance barrier, but it also has the disadvantage of expanding the surveillance area randomly.

In addition, the performance of Algorithm 1: *Random-Value-Camera-Level* and Algorithm 2: *ALL-Random-With-Weight* is summarized in Table I. As seen in Table I, it can be checked that both algorithms return adaptive activation according traffic volume increase and decrease with time variation for Graph 1: *Linear-Graph* and Graph 2: *Curvature-Graph*, which is definitely better than the static surveillance barrier without any adaptive strategy.

B. Complexity Analysis

If it is estimated for the time complexity of the proposed Algorithm 1: *Random-Value-Camera-Level* and Algorithm 2: *ALL-Random-With-Weight*, we use the given information of both algorithms, including the given areas S, a set of single lens camera C, and a set of activated set of single lens camera C_{act}. When both algorithms are considered with asymptotic perspective, assume that the total number of single lens camera is n, the total number of levels is q where $n > q$.

For the time complexity of Algorithm 1: *Random-Value-Camera-Level*, it identifies the traffic road space S within $O(1)$. Since a random value is assigned to every single lens camera for generation of random graph G, it takes $O(n)$. For selection of random value R, it takes $O(1)$. Then, for the calculation of scale factor in applying single camera in every level, it takes $q{\cdot}O(n)$. And, the transitioning into C_{act} and returning operation of C_{act} take$O(1)$. Accordingly, the total number of iterations will be $O(1)+O(n)+O(1)+q\cdot O(n)+O(n)+O(1)$. Because $O(1)$ and q are constants, an asymptotic upper bound is $O(n)$. The complexity of Algorithm 1: *Random-Value-Camera-Level* is $O(n)$.

For the time complexity of Algorithm 2: *ALL-Random-With-Weight*, it confirms the traffic road space S within $O(1)$. Because the random value is utilized to every single lens camera for creation of random graph G, it takes $O(n)$. When a random value R is chosen, it takes $O(1)$. About the weighted calculation of scale factor in single lens camera in each level of the traffic road space S, it takes $q\cdot O(n)$ consequently. The verifying time for the number of activated camera takes $O(n)$. Then, the transitioning into C_{act} and returning operation of C_{act} take $O(1)$. Consequently, the total number of iterations should be $O(1)+O(n)+O(1)+q\cdot O(n)+O(n)+O(1)$. Therefore, the complexity of Algorithm 2: *ALL-Random-With-Weight* is estimated as $O(n)$.

VI. CONCLUSION

In summary, this study introduced an innovative approach for augmented fluid surveillance using a group of single lens camera for urban traffic management, addressing the increasing need for adaptable traffic systems in smart cities. After the *MaxAugmentFluSurv* problem is formally defined, two different schemes were proposed with system initialization. Then, the performances of the devised methods were evaluated by earned outcomes through extensive experiments with various settings and scenarios, including different traffic volume, slope, and angle of camera. Since the proposed system only performed simulations own scenario through ad-hoc server, as future works, it is necessary to achieve augmented fluid surveillance through real-world traffic data to compare with existing critical methods and focus on time series data studies with deep learning.

REFERENCES

[1] S. Xu, J. Liu, N. Kato, and Y. Du, "Intelligent reflecting surface backscatter enabled multi-tier computing for 6G Internet of Things," *IEEE J. Sel. Areas Commun.*, vol. 41, no. 2, pp. 320–333, Feb. 2023.
[2] Q. Guo, F. Tang, and N. Kato, "Federated reinforcement learning-based resource allocation for D2D-aided digital twin edge networks in 6G Industrial IoT," *IEEE Trans. Ind. Informat.*, vol. 19, no. 5, pp. 7228–7236, May 2023.
[3] H. Guo, J. Li, J. Liu, N. Tian, and N. Kato, "A survey on space-air-ground-sea integrated network security in 6G," *IEEE Commun. Surveys Tuts.*, vol. 24, no. 1, pp. 53–87, 1st Quart., 2022.
[4] Q. Sha, X. Liu, and N. Ansari, "Efficient multiple green energy base stations far-field wireless charging for mobile IoT devices," *IEEE Internet Things J.*, vol. 24, no. 10, pp. 8734–8743, May 2023.
[5] S. Zhang, W. Liu, and N. Ansari, "Completion time minimization for data collection in a UAV-enabled IoT network: A deep reinforcement learning approach," *IEEE Internet Things J.*, vol. 72, no. 11, pp. 14734–14742, Nov. 2023.
[6] H. Ko, S. Pack, and V. C. M. Leung, "Performance optimization of serverless computing for latency-guaranteed and energy-efficient task offloading in energy-harvesting Industrial IoT," *IEEE Internet Things J.*, vol. 10, no. 3, pp. 1897–1907, Feb. 2023.
[7] D. Scotece, C. Fiandrino, and L. Foschini, "Handling data handoff of AI-based applications in edge computing systems," *IEEE Trans. Netw. Service Manag.*, vol. 20, no. 4, pp. 4435–4447, Dec. 2023.
[8] P. Bellavista, L. Foschini, R. Montanari, and N. Romandini, "FlowChain: The playground for federated learning in Industrial Internet of Things environments," *IEEE Internet Things Mag.*, vol. 5, no. 2, pp. 78–83, Jun. 2022.
[9] C. Boudagdigue, A. Benslimane, A. Kobbane, and J. Liu, "Trust-based certificate management for Industrial IoT networks," *IEEE Internet Things J.*, vol. 10, no. 14, pp. 12867–12885, Jul. 2023.
[10] A. Abouaomar, S. Cherkaoui, Z. Mlika, and A. Kobbane, "Resource provisioning in edge computing for latency-sensitive applications," *IEEE Internet Things J.*, vol. 8, no. 14, pp. 11088–11099, Jul. 2021.
[11] H. Xu, J. Wu, Q. Pan, X. Liu, and C. V. Verikoukis, "Digital twin and meta RL empowered fast-adaptation of joint user scheduling and task offloading for mobile Industrial IoT," *IEEE J. Sel. Areas Commun.*, vol. 41, no. 10, pp. 3254–3266, Oct. 2023.
[12] M. A. A. da Cruz, L. R. Abbade, P. Lorenz, S. B. Mafra, and J. J. P. C. Rodrigues, "Detecting compromised IoT devices through XGBoost," *IEEE Trans. Intell. Transp. Syst.*, vol. 24, no. 12, pp. 15392–15399, Dec. 2023.

Authorized licensed use limited to: Univ Of Incheon. Downloaded on November 08,2024 at 08:11:11 UTC from IEEE Xplore. Restrictions apply.

[13] V. Tuong, W. Noh, and S. Cho, "Sparse CNN and deep reinforcement learning-based D2D scheduling in UAV-assisted Industrial IoT networks," *IEEE Trans. Intell. Transp. Syst.*, vol. 20, no. 1, pp. 213–223, Jan. 2024.
[14] Y. Zhu, B. Mao, and N. Kato, "On a novel high accuracy positioning with intelligent reflecting surface and unscented Kalman filter for intelligent transportation systems in B5G," *IEEE J. Sel. Areas Commun.*, vol. 42, no. 1, pp. 68–77, Jan. 2024.
[15] M. Aledhari, M. Rahouti, J. Qadir, B. Qolomany, M. Guizani, and A. I. Al-Fuqaha, "Motion comfort optimization for autonomous vehicles: Concepts, methods, and techniques," *IEEE J. Sel. Areas Commun.*, vol. 11, no. 1, pp. 378–402, Jan. 2024.
[16] L. U. Khan, A. Elhagry, M. Guizani, and A. El-Saddik, "Edge intelligence empowered vehicular metaverse: Key design aspects and future directions," *IEEE Internet Things Mag.*, vol. 7, no. 1, pp. 120–126, Jan. 2024.
[17] D. Man, F. Zeng, J. Lv, S. Xuan, W. Yang, and M. Guizani, "AI-based intrusion detection for intelligence Internet of Vehicles," *IEEE Consum. Electron. Mag.*, vol. 12, no. 1, pp. 109–116, Jan. 2023.
[18] H. Ko, S. Pack, and V. C. M. Leung, "An optimal battery charging algorithm in electric vehicle-assisted battery swapping environments," *IEEE Trans. Intell. Transp. Syst.*, vol. 23, no. 5, pp. 3985–3994, May 2022.
[19] J. Chen et al., "Multiagent deep reinforcement learning for dynamic avatar migration in AIoT-enabled vehicular metaverses with trajectory prediction," *IEEE Internet Things J.*, vol. 11, no. 1, pp. 70–83, Jan. 2024.
[20] Y. Xiao et al., "Distributed traffic synthesis and classification in edge networks: A federated self-supervised learning approach," *IEEE Trans. Mobile Comput.*, vol. 23, no. 2, pp. 1815–1829, Feb. 2024.
[21] M. Xu et al., "Generative AI-empowered simulation for autonomous driving in vehicular mixed reality metaverses," *IEEE J. Sel. Topics Signal Process.*, vol. 17, no. 5, pp. 1064–1079, Sep. 2023.
[22] N. Z. Zenia, M. S. Kaiser, M. Mahmud, M. R. Ahmed, O. Kaiwartya, and J. Kamruzzaman, "REER-H: A reliable energy efficient routing protocol for maritime intelligent transportation systems," *IEEE Trans. Intell. Transp. Syst.*, vol. 24, no. 12, pp. 13654–13669, Dec. 2023.
[23] M. Maule, J. S. Vardakas, and C. V. Verikoukis, "A novel 5G-NR resources partitioning framework through real-time user-provider traffic demand analysis," *IEEE Syst. J.*, vol. 16, no. 4, pp. 5317–5328, Dec. 2022.
[24] J. Zheng et al., "Digital twin enabled task offloading for IoVs: A learning-based approach," *IEEE Trans. Netw. Sci. Eng.*, vol. 11, no. 1, pp. 659–672, Jan./Feb. 2024.
[25] C. He, T. H. Luan, R. Lu, Z. Su, and M. Dong, "Security and privacy in vehicular digital twin networks: Challenges and solutions," *IEEE Wireless Commun.*, vol. 30, no. 4, pp. 154–160, Aug. 2023.
[26] Y. Lee, T. Ha, A. Khreishah, W. Noh, and S. Cho, "Delay-controlled bidirectional traffic setup scheme to enhance the network coding opportunity in real-time Industrial IoT networks," *IEEE Internet Things J.*, vol. 10, no. 12, pp. 10559–10574, Jun. 2023.
[27] H. Otrok, M. Mehrandish, C. Assi, M. Debbabi, and P. Bhattacharya, "Game theoretic models for detecting network intrusions," *Comput. Commun.*, vol. 31, no. 10, pp. 1934–1944, 2008.
[28] K. Sarieddine, M. A. Sayed, D. Jafarigiv, R. Atallah, M. Debbabi, and C. Assi, "A real-time cosimulation testbed for electric vehicle charging and smart grid security," *IEEE Security Privacy*, vol. 21, no. 4, pp. 74–83, Jul./Aug. 2023.
[29] X. Yuan, S. Hu, W. Ni, X. Wang, and A. Jamalipour, "Deep reinforcement learning-driven reconfigurable intelligent surface-assisted radio surveillance with a fixed-wing UAV," *IEEE Trans. Inf. Forensics Security*, vol. 18, pp. 4546–4560, 2023.
[30] S. Hu, W. Ni, X. Wang, A. Jamalipour, and D. Ta, "Joint optimization of trajectory, propulsion, and thrust powers for covert UAV-on-UAV video tracking and surveillance," *IEEE Trans. Inf. Forensics Security*, vol. 16, pp. 1959–1972, 2021.
[31] J. Wang, X. Chang, J. V. Misic, V. B. Misic, and Y. Wang, "PASS: A parameter audit-based secure and fair federated learning scheme against free-rider attack," *IEEE Internet Things J.*, vol. 11, no. 1, pp. 1374–1384, Jan. 2024.
[32] H. Kang, X. Chang, J. V. Misic, V. B. Misic, J. Fan, and J. Bai, "Improving dual-UAV aided ground-UAV Bi-directional communication security: Joint UAV trajectory and transmit power optimization," *IEEE Internet Things J.*, vol. 71, no. 10, pp. 10570–10583, Oct. 2022.
[33] S. Lee, S. Lee, and H. Kim, "Differential security barriers for virtual emotion detection in maritime transportation stations with cooperative mobile robots and UAV," *IEEE Trans. Intell. Transp. Syst.*, vol. 24, no. 2, pp. 2461–2471, Feb. 2023.

Minsoo Kim (Student Member, IEEE) is currently pursuing the bachelor's and master's degree with the Department of Embedded Systems Engineering, Incheon National University, Incheon, South Korea.

He is a member of Intelligent Computing and Next Generation System Lab (ICONS), Incheon National University, with a keen interest in surveillance and dynamic barriers powered by deep learning. He is interested in solving real problem situations by applying deep learning techniques to the design of surveillance and barrier systems using embedded systems, such as cameras and UAVs.

Jalel Ben-Othman (Senior Member, IEEE) received the Ph.D. degree from the University of Versailles, Versailles, France, in 1998.

He is a Full Professor with the Université Paris-Saclay, Gif-sur-Yvette, France. His research interests are in the areas of wireless ad hoc and sensor networks, broadband wireless networks, the Internet of Things, and security in wireless networks in general and wireless sensor and ad hoc networks in particular. His work appears in highly respected international journals and conferences.

Hyunbum Kim (Senior Member, IEEE) received the Ph.D. degree in computer science from the University of Texas at Dallas, Richardson, TX, USA, in 2013.

He is currently an Associate Professor with the Department of Embedded Systems Engineering, Incheon National University, Incheon, South Korea and a lab founder of Intelligent Computing and Next Generation System Lab (ICONS). His research interests include algorithm design and performance analysis in various areas, including next generation frameworks, reinforced surveillance, intelligent transportation systems, sustainable computing, beneficial platforms, virtual emotion system, smart cities, and cyber security.

Authorized licensed use limited to: Univ Of Incheon. Downloaded on November 08,2024 at 08:11:11 UTC from IEEE Xplore. Restrictions apply.